Article

Not peer-reviewed version

Understanding Forage Palm Mucilage Behavior: Harnessing Plackett-Burman Screening for Tailoring Formulation and Process

Sander Moreira Rodrigues , Kaliston Aurélio Lomba , Tatiane Monteiro dos Santos , Gabrielly de Fátima Rodrigues das Neves , Maria Laura Gomes Vieira , Nathalia de Andrade Neves , César Alberto Roldán-Cruz , Giselle Pereira Cardoso , Silvia Leticia Rivero Meza , Polyanna Mara de Oliveira , Larissa de Oliveira Ferreira Rocha , Monalisa Pereira Dutra Andrade , Vivian Machado Benassi , Tatiana Nunes Amaral , Irene Andressa , Maria Teresa Pedrosa Silva Clerici , Marcio Schmiele *

Posted Date: 1 July 2025

doi: 10.20944/preprints202507.0021.v1

Keywords: apparent viscosity; hydrocolloids; proteins; rheology; salts; stability

Article

Understanding Forage Palm Mucilage Behavior: Harnessing Plackett-Burman Screening for Tailoring Formulation and Process

Sander Moreira Rodrigues [1,†], Kaliston Aurélio Lomba [1,†], Tatiane Monteiro dos Santos [1,†], Gabrielly de Fátima Rodrigues das Neves [1,†], Maria Laura Gomes Vieira [1,†], Nathália de Andrade Neves [1,†], Cesar Alberto Roldan-Cruz [3,†], Giselle Pereira Cardoso [1,†], Silvia Letícia Rivero Meza [4,†], Polyanna Mara de Oliveira [5,†], Larissa de Oliveira Ferreira Rocha [1,†], Monalisa Pereira Dutra Andrade [1,†], Vivian Machado Benassi [1,†], Tatiana Nunes Amaral [*,1,†], Irene Andressa [6,†], Maria Teresa Pedrosa Silva Clerici [7,†] and Marcio Schmiele [1,†]

1 Institute of Science and Technology, Federal University of Jequitinhonha and Mucuri Valleys, Minas Gerais, Brazil
2 Institute of Agrarian Sciences, Federal University of Jequitinhonha and Mucuri Valleys, Minas Gerais, Brazil
3 Faculty of Nutrition, Veracruz University, Veracruz, Mexico
4 Department of Agroindustrial Science and Technology, Federal University of Pelotas, Rio Grande do Sul, Brazil
5 Agricultural Research Company of Minas Gerais, Gorutuba Experimental Field, Minas Gerais, Brazil
6 Department of Food Technology, Federal University of Viçosa, Minas Gerais, Brazil
7 School of Food Engineering, University of Campinas, São Paulo, Brazil
* Correspondence: marcio.sc@ict.ufvjm.edu.br
† These authors contributed equally to this work.

Abstract

The rheological and textural behavior of gels containing forage palm mucilage (FPM) was investigated using the Plackett–Burman design and multivariate analysis. The influence of carbohydrates (xanthan gum, carboxymethyl cellulose, and sucrose), proteins (soy, egg, and whey), and salts (NaCl and $CaCl_2$), as well as pH and temperature, on FPM formulations was evaluated ($\alpha < 0.10$ and $R^2 > 0.75$). The flow curves indicate that gels fitted to Ostwald-de Waele model and presented pseudoplastic behavior. Chewing viscosity (at a shear rate of 10 s^{-1}) showed results between 0.05 and 36.16 $Pa \cdot s$, affected by xanthan gum, FPM and egg albumin. Hysteresis (−1138 to 3950 (Pa·s^{-1})) was reduced with increasing pH ($P = 0.041$), indicating the formation of more stable three-dimensional networks. Significant effects on firmness (0.114-0.434 N), consistency (1.286-3.397 N·s), cohesiveness (0.047-0.167 N), and viscosity index (0.067-0.810 N·s) were observed for sucrose, salts, and temperature ($P < 0.100$). Chemometric analysis confirmed the influence of these factors on the evaluated responses but revealed no correlation between rheological and textural parameters.

Keywords: apparent viscosity; hydrocolloids; proteins; rheology; salts; stability

1. Introduction

Forage palm (*Opuntia ficus-indica* Mill.) is a native cactus species of Mexico [1] that has been successfully grown in sustainable systems, showing high yields and low water and energy demands in the arid and semi-arid regions of Brazil. This species is considered a multipurpose plant for animal feed, fruit production, human consumption, biofuel dye production and cosmetic applications. Its structure consists of modified stems, known as cladodes, which are thick and succulent, serving as reservoirs for water and carbohydrates. The chemical composition of the cladodes varies according to edaphoclimatic conditions, agricultural management practices, species and plant age [2,3].

The *Sertânia* cultivar of forage palm, commonly referred to as *palma gigante*, is one of the most traditional and widely cultivated varieties in Brazil [4], accounting for more than 95% of palm plantations in the state of Pernambuco. This cultivar is distinguished by its high tolerance to water deficiency

 doi:10.20944/preprints202507.0021.v1

and its remarkable capacity to synthesize mucilage, a greenish, high-viscous substance secreted by the cladodes upon mechanical damage or pressure [5]. Plant-derived mucilage functions as a hydrocolloid and is valued for its hydrodynamic and surface properties, presenting potential applications in a wide range of food products [6].

Mucilages play a fundamental role in the food industry due to their rheological and technofunctional properties, including their thickening, emulsifying, stabilizing and gelling capabilities [7]. Due to these characteristics, mucilages are widely employed to modify the texture and viscosity of various food products, such as sauces, soups, desserts, ice creams, and frozen dough, where they also inhibit the formation of ice crystals [8]. In addition, they serve as gelling agents in jellies and confectionery products, providing structure and stability to the final formulations. Their emulsifying properties contribute to the homogenization of dispersed systems, making them essential components in the formulations of mayonnaise, sauces, and dairy products [9].

In baking applications, mucilages improve moisture retention, optimize texture, and extend the shelf life of gluten-free bread, cakes, and cookies [10]. They are also used as fat replacements and fiber sources in functional food formulations, helping to develop products with improved nutritional profiles [11]. Another notable application involves their use in edible coatings [12] for fruits, vegetables and cheeses, where they act as moisture barriers and delay oxidative processes [13,14]. In liquid food systems, including juices, plant-based beverages, and protein shakes, mucilages improve colloidal stability and improve sensory attributes, making them a promising additive for the food industry [15].

Plant-derived hydrocolloids have been extensively used in various industries, including the food, pharmaceutical, cosmetic, petroleum, textile, and paper sectors, because of their broad applicability, favorable technological properties (e.g., stability and functionality), and low production costs. These compounds belong to a diverse group of long-chain polymers, primarily composed of polysaccharides and proteins, distinguished by their ability to form gels and viscous dispersions in aqueous systems [16]. Hydrocolloids are metabolic products synthesized by plants that serve as energy and water storage materials while contributing to structural integrity and elasticity [17]. In most cases, they are classified as complex water-soluble polysaccharides, consisting predominantly of monosaccharide units [18].

The hydrodynamic and surface properties are widely utilized as thickening, stabilizing, emulsifying, and gelling agents, making them essential components in various formulations. Incorporation of these compounds is recognized to enhance the functional characteristics of products by improving properties such as gelation, solution thickening, and stability in emulsions, foams, and dispersions [19]. The technological attributes of plant mucilage allow its successful application in the food industry, particularly in products that require gelation, a soft texture, and enhanced juiciness [20].

Furthermore, mucilages have emerged as promising biopolymers in 3D food printing due to their rheological and structural properties, which facilitate extrusion and maintain the integrity of the deposited layers [21]. Their thickening and gelling capacities contribute to increased viscosity and cohesion in formulations, ensuring controlled flow through the extrusion nozzle while preserving the structural stability of printed products. Furthermore, mucilages act as stabilizing and emulsifying agents, enabling the homogeneous incorporation of ingredients and improving the sensory attributes of foods. Their application is particularly relevant in the formulation of customized food products, including those enriched with fibers, proteins, and bioactive compounds, offering nutritional and functional benefits [22,23]. In addition, they have been explored to develop innovative textures and replace synthetic ingredients, providing a sustainable alternative for high-value-added printed foods [24].

Gels are semi-rigid three-dimensional networks formed through the interaction of biopolymers, capable of retaining large amounts of water or other liquid substances. Gel formation typically involves carbohydrates, proteins, and salts [25]. Carbohydrates, such as polysaccharides (pectin, agar, xanthan gum, or guar gum), play a crucial role in the structure of the gel network through hydrogen bonding and hydrophobic interactions [26]. Proteins, including collagen and albumin, contribute to

 doi:10.20944/preprints202507.0021.v1

network formation through denaturation and crosslinking processes, in which gelation begins with the unfolding of protein molecules due to heating, pH alterations, or mechanical agitation, followed by their aggregation into a cohesive three-dimensional matrix [27].

Salts, particularly divalent ions such as calcium (Ca^{2+}), enhance gel formation by stabilizing the polymer network through ionic interactions, as observed in pectin gelation under acidic conditions. This mechanism is influenced by the concentration, pH and temperature of the components, which regulate the strength and nature of intermolecular interactions [28]. The synergistic interaction among these components improves gel stability and mechanical properties [29]. For instance, in protein-polysaccharide systems, gel formation is governed by structural compatibility and the balance between attractive and repulsive molecular forces. In mixed solutions, salts modulate electrostatic charge, reducing repulsion between charged molecules, thereby promoting aggregation and the formation of denser networks. Studies have indicated that fine-tuning physicochemical conditions is crucial for controlling gel texture and functionality, with applications ranging from food products to biomaterials [30,31].

Against this backdrop, the present study aimed to evaluate the rheological and textural behaviors of applying FPM in model gels using an exploratory experimental design based on the Plackett-Burman approach. The effects of different formulations were analyzed, considering treatments with different pHs, temperatures, and concentrations of carbohydrates, proteins, salts, and FPM.

2. Materials and Methods

The use of forage palm for scientific investigation was registered under the number AF2C488 in the National System for the Management of Genetic Heritage and Associated Traditional Knowledge (SisGen) of the Ministry of Environment of the Federative Republic of Brazil.

2.1. Raw Materials and Additives

The raw materials used in this study included forage palm (*Sertânia* variety), commercial sucrose (Guarani), xantan gum - XG (Soldiers Nutrition), carboxymethyl cellulose with 90% purity - CMC (Adicel), commercial iodized sodium chloride (Cisne), dihydrated calcium chloride (Perfyl Tech), egg albumin with a minimum protein content of 78% (NaturaOvo), soy protein isolate with a minimum protein content of 90% - SPI (Growth Supplements), whey protein with a minimum protein content of 90% (Growth Supplements), citric acid (Dinâmica), and sodium carbonate (Dinâmica).

The selection of raw materials and additives for the experiment was based on their widespread application in food formulation and processing and their relevance to the chemical composition and techno-functional properties of food systems. Additionally, their use in diverse food applications justified their inclusion, facilitating a comprehensive assessment of their interactions and effects within the scope of this study.

The forage palm cladodes, approximately one year old, were donated by the Minas Gerais Agricultural Research Company (EPAMIG) from the experimental field of Acauã (Leme do Prado, Minas Gerais, Brazil; 17°07’37"S, 42°46’02"W) in December 2023. The mucilage was extracted from these cladodes and used as the primary raw material for the analyzes carried out in the present study. The proximate composition of FPM was determined according to the methods of the Association of Official Analytical Chemists[32], including moisture (method 930.04), protein (method 940.26; conversion factor N = 6.25), lipid (method 948.22), mineral (method 920.152) and total carbohydrates (method 2020.07-2020) contents.

In addition to FPM, the carbohydrates included in this study were sucrose, XG, and CMC. Sucrose was selected because of its ubiquitous presence in food matrices, where it functions as a sweetening agent, contributes to the body of liquid foods, and influences the texture of semi-solid or solid products. Its multifunctional role is crucial in defining the physical structure and overall quality of various food formulations [33]. XG and CMC were included due to their well-established functional properties, particularly their thickening, stabilizing, and gelling capacities, which are essential for modulating rheological behavior and ensuring the stability of the food system [34,35].

 doi:10.20944/preprints202507.0021.v1

The salts used in this study were commercial grade iodized sodium chloride and dihydrated calcium chloride. Sodium chloride was selected for its monovalent ionic nature and its common application in food systems, where it plays a fundamental role in flavor enhancement, physicochemical modification, rheological adjustment and preservation [36]. Calcium chloride, a divalent salt, was chosen for its structural and stabilizing functions, particularly its ability to promote cross-linking in food matrices, thus improving texture and product stability [37].

The protein sources used in this study included whey protein, egg albumin, and SPI, as they are commercially available, food-grade, and obtained from online suppliers. The whey protein was selected due to its well-documented functional properties, including high solubility, foaming capacity, and gelling ability, which make it widely applicable in various food formulations [38]. Egg albumin was chosen for its foaming and stabilizing properties and relevance in formulations requiring structural integrity and textural control [39]. Finally, SPI was incorporated because of its technological and nutritional attributes, including its emulsifying and gel-forming capacities, as well as its high protein content, which makes it a valuable ingredient in diverse food applications, particularly in meat and dairy analogs. [40]

2.2. Plackett-Burman Screening Design

The Plackett-Burman exploratory experimental design was selected due to its widespread application as a statistical tool to identify the most influential factors within a system, considering both process and formulation parameters [41]. This design was implemented with 11 independent variables distributed in 16 trials and three additional repetitions at the central point, resulting in 19 trials. Each variable was assessed at two levels: minimum (-1) and maximum (+1). The actual and coded levels assigned to each variable are presented in Table 1. A final mass of 180 g was established to ensure the feasibility of all analyses performed on the developed gel, standardized with distilled water in all trials.

Table 1. Independent variables and real levels for the trials.

Trials	X_1	X_2	X_3	X_4	X_5	X_6	X_7	X_8	X_9	X_{10}	X_{11}
1	25	0.05	0.05	0.2	1.00	0.05	0.2	2.0	2.0	3.0	75
2	25	3.00	0.05	0.2	0.05	1.00	0.2	0.2	2.0	8.0	25
3	25	3.00	3.00	0.2	0.05	0.05	2.0	0.2	0.2	8.0	75
4	25	3.00	3.00	15.0	0.05	0.05	0.2	2.0	0.2	3.0	75
5	1	3.00	3.00	15.0	1.00	0.05	0.2	0.2	2.0	3.0	25
6	25	0.05	3.00	15.0	1.00	1.00	0.2	0.2	0.2	8.0	25
7	1	3.00	0.05	15.0	1.00	1.00	2.0	0.2	0.2	3.0	75
8	25	0.05	3.00	0.2	1.00	1.00	2.0	2.0	0.2	3.0	25
9	25	3.00	0.05	15.0	0.05	1.00	2.0	2.0	2.0	3.0	25
10	1	3.00	3.00	0.2	1.00	0.05	2.0	2.0	2.0	8.0	25
11	1	0.05	3.00	15.0	0.05	1.00	0.2	2.0	2.0	8.0	75
12	25	0.05	0.05	15.0	1.00	0.05	2.0	0.2	2.0	8.0	75
13	1	3.00	0.05	0.2	1.00	1.00	0.2	2.0	0.2	8.0	75
14	1	0.05	3.00	0.2	0.05	1.00	2.0	0.2	2.0	3.0	75
15	1	0.05	0.05	15.0	0.05	0.05	2.0	2.0	0.2	8.0	25
16	13	1.52	1.52	7.6	0.51	0.51	1.1	1.1	1.1	5.5	50
17	13	1.52	1.52	7.6	0.51	0.51	1.1	1.1	1.1	5.5	50
18	13	1.52	1.52	7.6	0.51	0.51	1.1	1.1	1.1	5.5	50
19	13	1.52	1.52	7.6	0.51	0.51	1.1	1.1	1.1	5.5	50

X_1 - Forage palm mucilage (%), X_2 - NaCl (%), X_3 - $CaCl_2$ (%), X_4 - Sucrose (%), X_5 - Xanthan gum (%), X_6 - Carboxymethyl cellulose (%), X_7 - Whey protein (%), X_8 - Egg albumin (%), X_9 - Soy protein isolate (%), X_{10} - pH, X_{11} - Temperature (°C). Total mass was adjusted to 100 % with distilled water. Levels determined by the authors according to [41].

2.3. Gels Development

The forage palm cladodes were manually selected and any signs of damage were discarded. The selected cladodes were then washed with potable water to remove surface impurities and sanitized

 doi:10.20944/preprints202507.0021.v1

in NaClO (200 ppm) solution for 15 min. To remove residual chlorine, they were rinsed with potable water. The gloquides were manually removed with a knife, after which the cladodes were packaged in high-density polyethylene bags and stored in a freezer (Consul, Joinville, Brazil) at -18 ° C until further use. An overview of the gel preparation and evaluation process is presented in Figure 1.

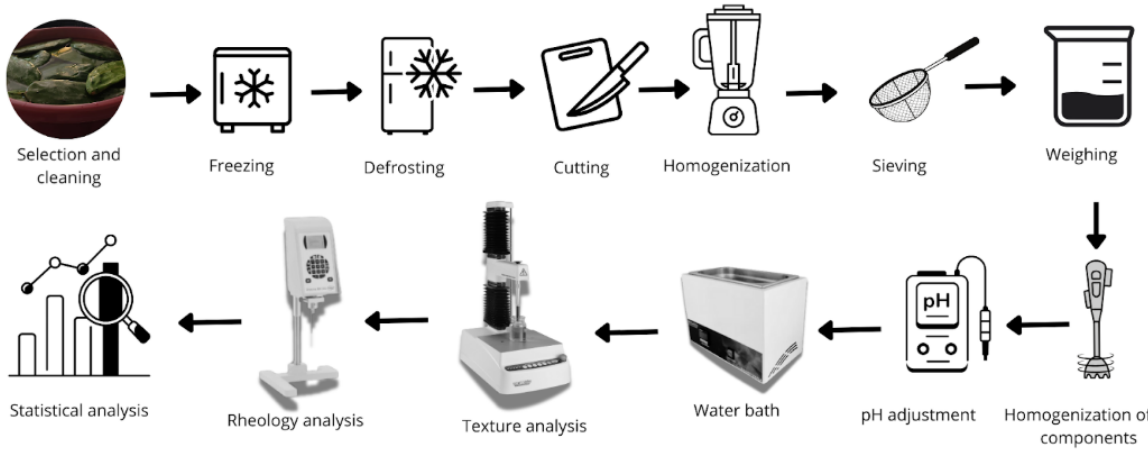

Figure 1. Flowchart of gel preparation.

For processing, the forage palm cladodes were thawed at 7 °C for 24 h in a cold chamber (BF Cozinhas, São Paulo, Brazil). After thawing, they were cut manually along the longitudinal section and subjected to manual mucilage extraction. Approximately 100 g of mucilage were homogenized using a high-speed industrial blender (Lar-2, Metal Ferreira, So Paulo, Brazil), ensuring uniformity. The homogenized mucilage was then passed through a 1 mm mesh sieve to remove larger fibers, facilitating its suitability for subsequent experimental procedures.

The quantities of each independent variable were measured precisely using an analytical balance (AUY 220 Shimadzu, Piracicaba, Brazil). For gel preparation, the dry components were first dissolved in 50 g of distilled water and homogenized using an Ultraturrax TE-102 (Turratec, Piracicaba, Brazil) at 4000 rpm. The FPM was then incorporated into the mixture and manually homogenized with a glass rod. The pH of the solution was adjusted according to the experimental design using a pH meter (mPA210 Tecnopon, Piracicaba, Brazil) with saturated solutions of sodium bicarbonate and/or citric acid. The total mass was then adjusted to 180 g with distilled water, followed by additional manual homogenization. As specified for the experimental design, the mixture was equilibrated for 1 h at the designated temperature in a water bath (SL150 Solab, Piracicaba, Brazil). Finally, the prepared sample was subjected to rheological and instrumental texture analysis.

2.4. Rheological Behavior

The rheological properties of the samples were evaluated using a shear rheometer (RM-200 Rheomat, Lamy Rheology, Champagne au Mont d'Or, France) to obtain flow curves and determine the apparent viscosity, thereby characterizing the rheological behavior of the gels. Approximately 20 g of each gel sample were analyzed in individual trials using the MK-DIN No. 2 spindle and the DIN 2 TUBE measuring system. The shear rate sweep was performed in two stages: an ascending ramp from 5 to 100 s^{-1}, followed by a descending profile from 100 to 5 s^{-1}, with shear rate increments applied every 5 seconds, totaling 15 minutes of testing at room temperature (23 $\pm$ 1 °C).

Several rheological models were tested to describe the flow behavior, including the Newtonian, power law (Ostwald-de Waele), Casson, and Bingham models. Based on the highest regression coefficient (r = 0.9852), the Ostwald-de Waele model was selected as the best fit. The data collected included shear rate, shear stress, and apparent viscosity, which were used to generate flow curves. In this context, the consistency index (k) was adopted as a primary response variable, while the flow behavior index (n) was not statistically analyzed, serving solely to confirm the fit of the model.

 doi:10.20944/preprints202507.0021.v1

Furthermore, apparent viscosity (at a shear rate of 10 s^{-1}) [42] and the hysteresis loop areas (Pa·s^{-1}) were also adopted as response variables to assess structural and flow properties.

2.5. Instrumental Texture

Instrumental texture analysis was performed using a TA-XT Plus texture analyzer (Micro Systems Stable, Haslemere, England). An acrylic disc with a diameter of 35 mm and a thickness of 6 mm was utilized for the analysis, together with a 50 mm high extrusion pot. The gel samples were carefully placed inside the container to a uniform height of 25 mm to ensure the standardization of the experimental conditions. Texture analysis was performed under the following conditions: pre-test, test, and post-test speeds of 1 mm·s^{-1}; probe height of 70 mm; detection force of 0.1 N; 25 kg load cell; compression distance corresponding to 30% of the initial sample height and at room temperature (23± 1 °C). All measurements were performed in quadruples. The parameters evaluated included firmness (N), consistency (N·s), cohesiveness (N), and viscosity index (N·s).

2.6. Statistical Analysis

The hypersis loop areas were determined using Origin 2019 software. Data were obtained in quadruples for each trial and normality was assessed using the Shapiro-Wilk test ($P < 0.05$). The results were analyzed using the Response Surface Methodology in Statistica 7.0 software, with a confidence level of 90% ($P < 0.10$) and a minimum coefficient of determination of 75% [41]. For multivariate analysis, heatmap evaluation, principal component analysis (PCA), and partial least squares discriminant analysis (PLS-DA) were conducted using the experimental data. Pearson's correlation coefficient was applied to assess overall variability among dependent variables using MetaboAnalyst 5.0 software [43].

3. Results and Discussions

3.1. Proximate Composition

The FPM was characterized by a high moisture content (96.06 ± 0.33%) [44]. Regarding total solids, the protein content was 7.68 ± 0.38%, highlighting the presence of this nitrogenous compound in the mucilage. The ether extract amounted to 2.26 ± 0.43%, consisting of saponifiable and unsaponifiable material, while minerals accounted for 26.29 ± 4.03%. Consequently, the total carbohydrate content was determined to be 63.77%.

3.2. Rheological Behavior

The rheological analysis, performed using a shear rheometer, included ascending and descending shear rate ramps, from which the hysteresis loop area was calculated. This parameter provides valuable information on the structural breakdown and recovery behavior of the samples under shear. The ascending ramp was associated with an increase in viscosity with the gradual application of the shear rate. In contrast, the viscosity of the gel progressively decreased with an increase in shear rate, exhibiting pseudoplastic behavior. This phenomenon can be attributed to the orientation and structural rearrangement of the gel particles under the influence of shear forces, leading to a reduction in flow resistance and a thinning of the medium. Table 2 presents the average results for viscosity in chewing, hysteresis, consistency index (k) and flow behavior index (n). The flow behavior index (n) values obtained for all trials were less than 1, confirming a pseudoplastic behavior consistent with shear-thinning fluids.

 doi:10.20944/preprints202507.0021.v1

Table 2. Apparent viscosity data and rheological behavior for the gels in the Plackett-Burman screening design trials.

Trials	Viscosity in chewing - 10 s^{-1} (Pa· s)	Hysteresis (Pa·s^{-1})	Consistency index (k)	Flow behavior index (n)
1	36.16 ± 2.85	3950	225.64 ± 33.62	0.21 ± 0.03
2	4.51 ± 0.24	580	11.15 ± 0.81	0.55 ± 0.07
3	2.35 ± 0.35	48	12.74 ± 2.72	0.26 ± 0.04
4	1.61 ± <0.01	256	6.54 ± 3.98	0.29 ± 0.10
5	10.73 ± 0.97	708	59.48 ± 6.50	0.28 ± 0.05
6	21.53 ± 2.40	-590	115.57 ± 1.15	0.30 ± 0.02
7	16.40 ± 1.88	109	72.90 ± 2.26	0.38 ± 0.04
8	27.75 ± 1.24	528	122.42 ± 3.56	0.31 ± 0.02
9	10.67 ± 0.98	992	28.53 ± 3.24	0.50 ± 0.03
10	18.57 ± 0.45	80	112.05 ± 2.67	0.17 ± 0.04
11	6.32 ± 1.44	-1138	15.48 ± 2.60	0.48 ± 0.15
12	14.00 ± 0.29	-361	81.34 ± 3.35	0.24 ± 0.03
13	14.47 ± 1.73	-575	69.74 ± 4.41	0.21 ± 0.14
14	2.09 ± 0.26	199	3.31 ± 0.07	0.71 ± 0.07
15	0.104 ± <0.01	14	0.31 ± 0.20	0.43 ± 0.13
16	0.05 ± <0.01	21	44.21 ± 1.01	0.31 ± 0.03
17	5.25 ± 0.21	294	18.49 ± 1.30	0.41 ± 0.03
18	6.14 ± 0.27	387	21.42 ± 1.00	0.41 ± 0.02
19	6.82 ± 0.27	368	23.99 ± 2.28	0.37 ± 0.02

Viscosity in chewing. Viscosity is a property related to the texture of materials, defined as the resistance that a fluid offers to movement when subjected to force. This characteristic is typically evaluated through flow tests. Viscosity is closely associated with mastication, as during the chewing process, food experiences mechanical forces such as shear and compression applied by the teeth, tongue, and jaw muscles. The resistance of the food to these forces is influenced by its viscosity, especially in semi-solid foods. Studies have shown that the shear rate during mastication varies considerably, making it impractical to evaluate on the basis of a single fixed value. Instead, the shear rate should be determined within a range of values that represent the actual conditions. Among the suggested ranges, apparent viscosity at a shear rate of 10 s^{-1} has been widely used as an estimate to simulate the forces applied during mastication of moderately firm foods [45].

The viscosity analysis was designed to identify the factors that exert the greatest influence on the rheological properties of the system. The viscosity values ranged from 0.05 to 36.16 $Pa \cdot s$, as shown in Table 2. The greatest effect on mastication viscosity was attributed to the presence of XG (19.49 $Pa \cdot s$; $P < 0.001$), followed by FPM (6.23 $Pa \cdot s$; $P < 0.038$) and egg albumin (5.50 $Pa \cdot s$; P < 0.058). This behavior is illustrated in the Pareto chart (Figure 2(A)). The data set was considered satisfactory by ANOVA, with a coefficient of determination of 92.42%, a $F_{calc}/F_{tab(12;6;0.10)}$ ratio of 2.10, and a P-value of 0.018.

 doi:10.20944/preprints202507.0021.v1

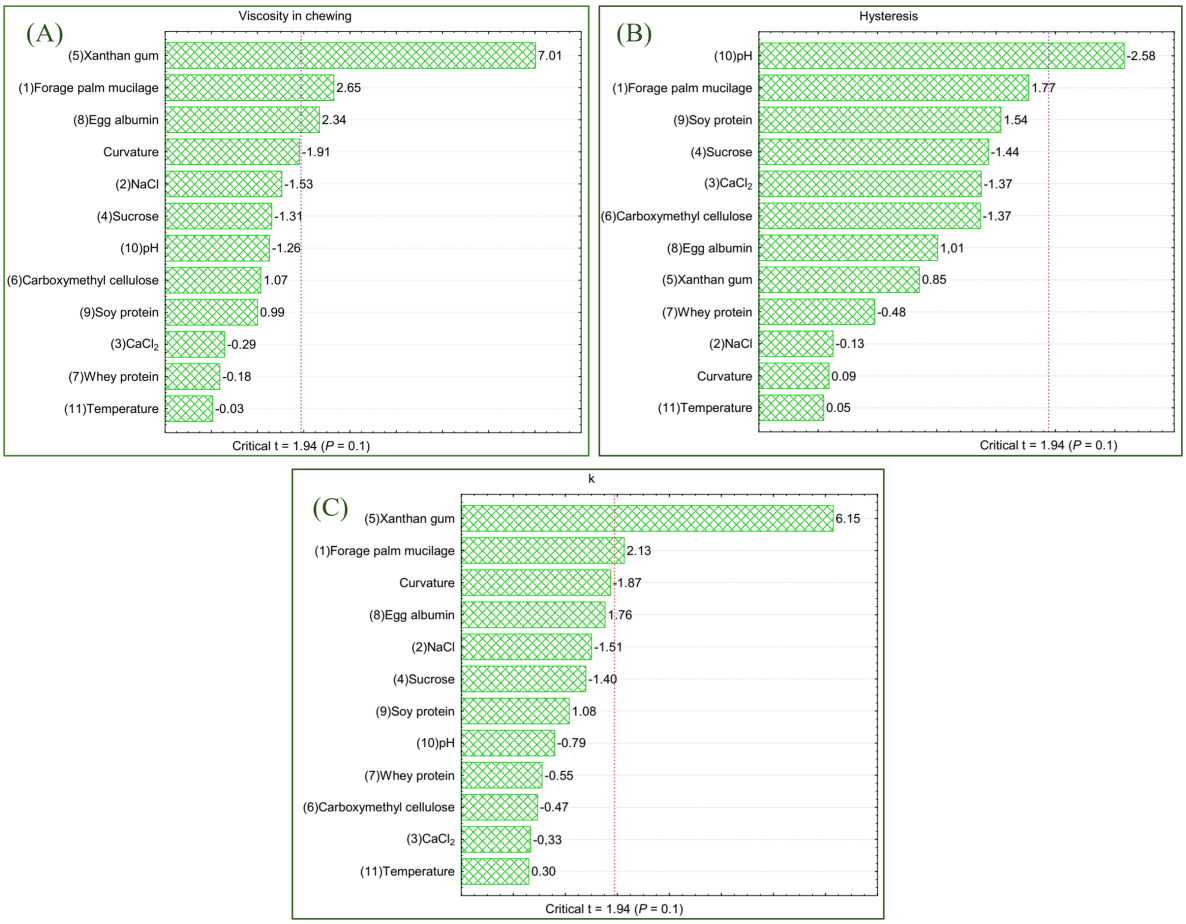

Figure 2. Estimated effects for the independent variables on the consistency index k (A), hysteresis (B) and Viscosity in chewing - 10 s^{-1} (C) represented by the Pareto chart.

Hysteresis. Hysteresis refers to the rheological phenomenon that describes the behavior of a gel during the application and removal of an external force, such as shear [46]. Lower hysteresis indicates the faster and more efficient ability of a gel to reorganize after being subjected to shear force [47]. This dependent variable ranged from -1138 to 3950 Pa $\cdot$ s^{-1}, with pH being the only independent variable that significantly affects the response under analysis (-1088 Pa $\cdot$ s^{-1}; P = 0.041). This behavior is illustrated in the Pareto chart (Figure 2(B)). ANOVA showed a coefficient of determination of 76.90% and a significance level of 0.018. The F_{calc} value was 0.57 times lower than $F_{tab(12;6;0.10)}$ and a significant lack of fit was observed (P = 0.002), indicating that the variability of the results could not be fully explained by the statistical model.

Trials #6, #11, #12, and #13 presented negative hysteresis values, indicating that the area under the descending ramp was greater than that under the ascending ramp. All of these trials shared the maximum pH value (+1 = 8.0, in coded and real values).

Consistency index Consistency index (k) derived from the power-law model and quantifies the intrinsic viscous strength of gel systems by expressing the relationship between shear stress and shear rate. In practice, K approximates the apparent viscosity at a shear rate of 1 s^{-1} and reflects the internal resistance of the network structure to deformation. Higher (k) values indicate stronger gel matrices, often resulting from increased hydrocolloid concentration or enhanced polymer-polymer interactions. This index is directly related to the textural and processing attributes of food gels, such as creaminess and pumpability [48]. As such, (k) provides a meaningful parameter for comparing formulation effects and evaluating gel robustness under low-shear conditions.

The consistency index values ranged from 0.31 to 225.64 (Table 2), with XG (97.61; $P < 0.001$) the significant factor to the (k) increasing. This behavior is illustrated in the Pareto chart (Figure 2(C)).

 doi:10.20944/preprints202507.0021.v1

The data set was considered satisfactory by ANOVA, with a coefficient of determination of 86.62%, a $F_{calc}/F_{tab(12;6;0.10)}$ ratio of 1.60, and a P-value of 0.035.

Discussion on the rheological behavior of gels. The independent variables that exerted the greatest influence on the apparent viscosity and rheological behavior of the gels were XG, FPM, CMC, and egg albumin, with pH also affecting gel hysteresis. The differences in rheological behavior across various experiments can be observed in Figure 3: (A) for trial #4, (B) for trial #6, (C) for trial #11, and (D) for trial #19. The emphasized carbohydrates possess high molecular weights and strong water affinity through hydrogen bonding. XG, a biopolymer produced by gram-negative bacteria of the genus *Xanthomonas*, features a primary structure made up of repeating pentasaccharide units. The linear chain consists of two β-(1→4)-D-glucose units, while the trisaccharide branches contain two units of mannose and one unit of glucuronic acid. In about half of the terminal D-mannose units, a pyruvic acid residue is attached at positions 4 and 6, and the nonterminal D-mannose unit carries an acetyl group at position 6 [49]. This chemical structure results in a broad molecular mass range (between 2×10^6 and 20×10^6 Da), allowing XG to form highly viscous solutions that exhibit gel-like properties even at relatively low concentrations. When added to aqueous food products, XG promotes the formation of stable, cohesive gels, improving viscosity and improving the rheological characteristics of the system [50,51]. This behavior is attributed to the ability of XG to form a three-dimensional network through interactions with water molecules, resulting in rheological stability [52,53].

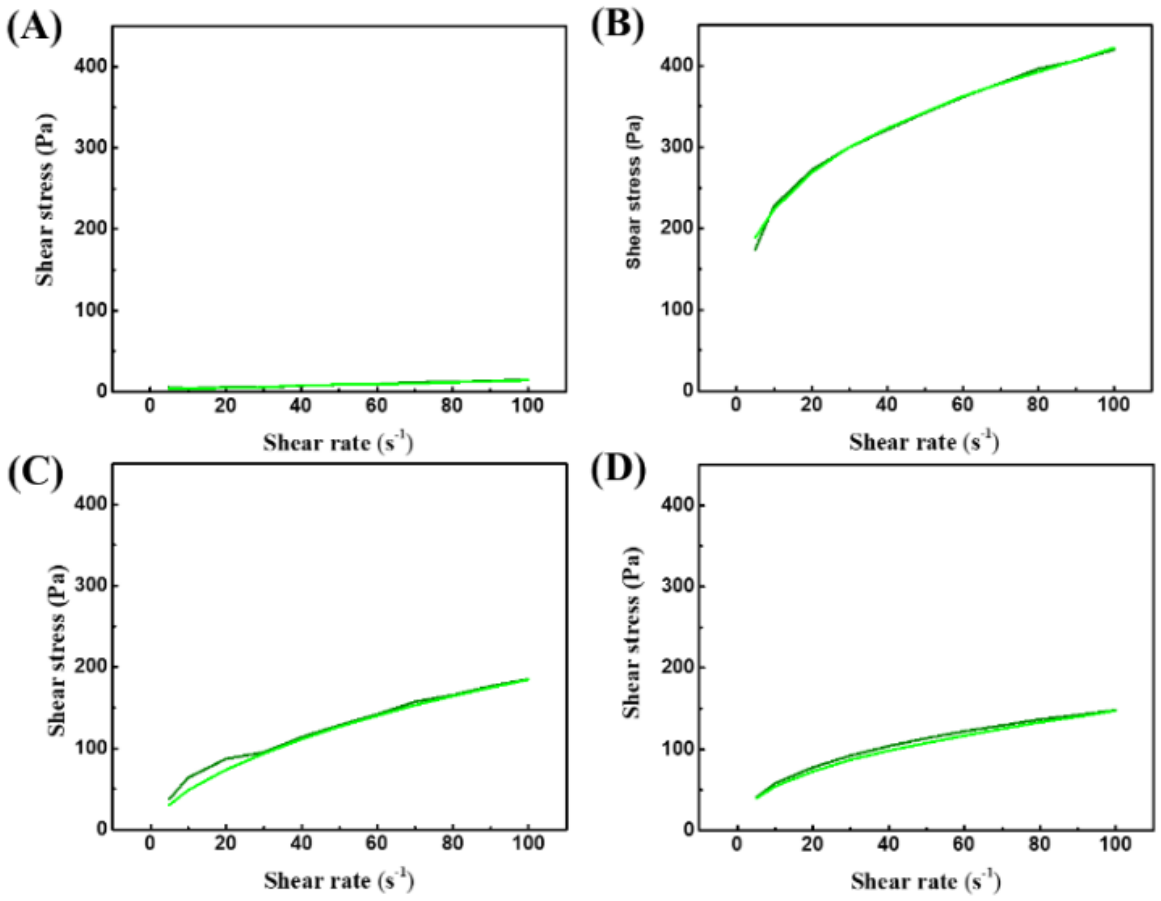

Figure 3. Flow curves for visualization of the ascending (—) and descending (—) ramps of trials 4 (A), 6 (B), 11 (C) and 19 (D) of the Placket-Burman screening design.

CMC, a cellulose derivative substituted with carboxymethyl groups, is an anionic polyelectrolyte that induces the attraction of depletion in gels [54]. A higher degree of substitution of the CMC results in a higher endogenous charge density, reducing the crystallinity of the structure and promoting the formation of hydrogen bonds between the polymer and water. Furthermore, carboxymethylcellulose interactions with other components can work synergistically to structure food gels [55,56].

 doi:10.20944/preprints202507.0021.v1

FPM is primarily composed of dietary fibers, with approximately 45 to 50% being soluble fiber and 50 to 55% insoluble fiber. The primary monomers in FPM are L-rhamnose (predominantly 50%), L-arabinose, D-galactose, and D-galacturonic acid (at intermediate concentrations of 10–20%), with lower amounts of D-mannose and D-xylose (<10%) [1,3]. The chemical structure of FPM consists of a highly branched anionic polysaccharide complex, featuring numerous hydrophilic groups, particularly hydroxyls, carboxyls, and uronic [57].

Egg albumin is rich in sulfur-containing amino acids [58], which are responsible for forming disulfide bonds and other covalent bonds that contribute to the formation of gel structures when heated [59]. Additionally, egg albumin's high solubility, particularly at pH levels near or above neutrality, led to its reduced effect on the ascending and descending phases. Electrostatic interactions between proteins and proteins and salt may also have contributed to this behavior [60].

The positive effect of pH on gel hysteresis may be linked to the ionization of anionic polysaccharide groups, which promotes hydrogen bond formation with water and mild electrostatic repulsion between polysaccharides. This increases steric hindrance to aggregate formation and allows for water retention in the gel [61,62]. Furthermore, proteins exhibit higher solubility at pH values further away from their isoelectric point, which ranges from 4.6 to 4.9 for egg albumin [63]. Greater protein solubility increases the exposure of peptide bonds for the formation of hydrogen bonds, as well as for certain neutral amino acids such as serine, threonine, and tyrosine [64]. Furthermore, electrostatic interactions with acidic and basic amino acids [65], along with hydrophobic interactions with the side chains of nonpolar amino acids, further influence the properties of the gel [66,67].

3.3. Instrumental Texture

The texture of foods is a key modifiable factor that can promote consumer health and significantly influence taste preferences and general product acceptability [68]. This characteristic is directly affected by physical properties such as firmness, consistency, cohesiveness, and viscosity, which influence both tactile perception and chewing behavior during consumption. In addition, texture is closely related to food formulation and processing, with components such as polysaccharides, proteins, and lipids playing crucial roles in determining the structure and molecular interactions of the product. The data obtained from the instrumental texture analysis, which evaluated firmness, consistency, cohesiveness, and viscosity in the experimental design trials, are presented in Table 3.

Table 3. Instrumental texture data for gels from Plackett-Burman screening design trials.

Trial	Firmness (N)	Consistency (N·s)	Cohesiveness (N)	Viscosity index (N·s)
1	0.349 ± 0.014	2.783 ± 0.176	0.138 ± 0.006	0.734 ± 0.092
2	0.129 ± 0.002	1.300 ± 0.044	0.055 ± 0.001	0.088 ± 0.010
3	0.223 ± 0.009	1.598 ± 0.121	0.069 ± 0.003	0.145 ± 0.016
4	0.118 ± 0.003	1.286 ± 0.087	0.051 ± 0.002	0.071 ± 0.010
5	0.221 ± 0.016	1.801 ± 0.199	0.084 ± 0.002	0.237 ± 0.026
6	0.373 ± 0.016	2.582 ± 0.387	0.146 ± 0.003	0.616 ± 0.084
7	0.164 ± 0.015	1.397 ± 0.128	0.067 ± 0.004	0.160 ± 0.032
8	0.434 ± 0.022	3.397 ± 0.262	0.167 ± 0.004	0.810 ± 0.047
9	0.167 ± 0.001	1.325 ± 0.058	0.067 ± 0.001	0.149 ± 0.018
10	0.414 ± 0.020	2.898 ± 0.320	0.159 ± 0.004	0.692 ± 0.090
11	0.145 ± 0.001	1.313 ± 0.132	0.065 ± 0.003	0.106 ± 0.011
12	0.320 ± 0.010	2.023 ± 0.279	0.123 ± 0.005	0.402 ± 0.073
13	0.218 ± 0.027	1.754 ± 0.319	0.092 ± 0.003	0.399 ± 0.065
14	0.115 ± 0.001	1.338 ± 0.131	0.047 ± 0.005	0.067 ± 0.007
15	0.116 ± 0.001	1.664 ± 0.146	0.054 ± 0.002	0.085 ± 0.008
16	0.126 ± 0.011	1.466 ± 0.044	0.052 ± <0.001	0.070 ± 0.005
17	0.165 ± 0.002	1.571 ± 0.174	0.065 ± 0.003	0.163 ± 0.012
18	0.151 ± 0.004	1.425 ± 0.035	0.062 ± 0.001	0.127 ± 0.018
19	0.170 ± 0.006	1.508 ± 0.078	0.068 ± <0.001	0.165 ± 0.012

Values corresponding to the arithmetic mean of 4 repetitions ± standard deviation.

 doi:10.20944/preprints202507.0021.v1

Firmness and consistency. The firmness of the gels ranged from 0.114 to 0.434 N, with 96.89% of the variation explained by ANOVA. The F_{calc} value was 5.37 times higher than $F_{tab(12;6;0.10)}$ (P = 0.001). Except for pH, CMC, and soy protein, all other variables showed an influence on this dependent variable. XG had the greatest effect on gel firmness (0.169 N; P < 0.001), followed by FPM (0.074 N; P = 0.004) and bivalent salt ($CaCl_2$: 0.058 N; P = 0.013). Sucrose, temperature, sodium chloride, egg albumin, and whey protein also exhibited significant standardized effects, as illustrated in Figure 4 (A).

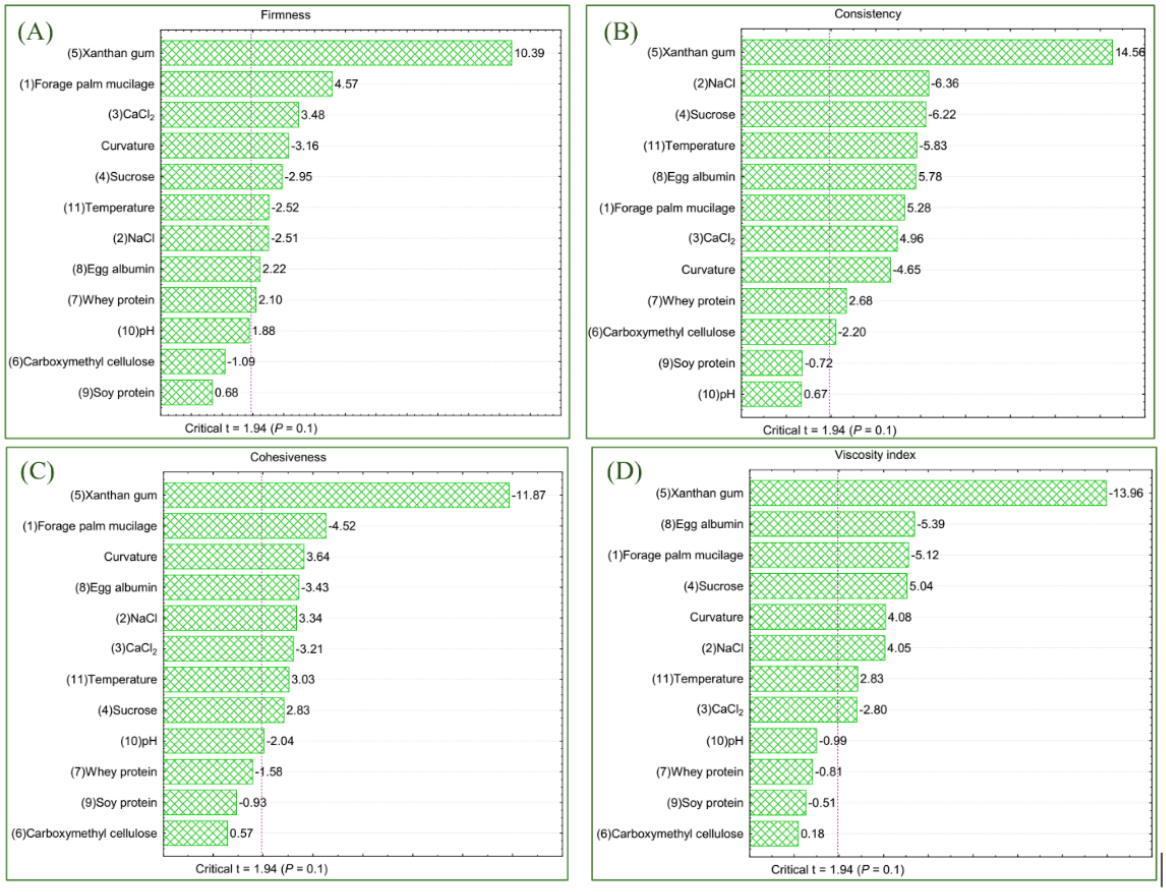

Figure 4. Estimated effects for the independent variables: firmness (A), consistency (B), cohesiveness (C), and viscosity index (D) represented by the Pareto chart.

The consistency of the gel ranged from 1.286 to 3.397 N·s in the trials, XG being the primary influencer (0.918 N·s; P < 0.001), followed by egg albumin (0.365 N·s; P = 0.001), FPM (0.333 N·s; P = 0.002), calcium chloride (0.313 N·s; P = 0.003), and whey protein (0.169 N·s; P = 0.036). Negative significant effects were observed with sodium chloride (−0.401 N·s; P = 0.001), sucrose (−0.393 N·s; P = 0.001), temperature (−0.368 N·s; P = 0.001), and carboxymethylcellulose (−0.139 N·s; P = 0.069). The standardized effects of the independent variables are shown in Figure 4 (B). The data set was considered satisfactory, with a determination coefficient of 98.67%, a $F_{calc}/F_{tab(12;6;0.10)}$ ratio of 12.80, and a P-value below 0.001, indicating an error rate of less than 0.1%.

Cohesiveness and viscosity index. The cohesiveness data ranged from 0.047 to 0.167 N, exhibiting a similar trend as observed for firmness. The greatest effect was observed with XG (0.064 N; $P < 0.001$) and FPM (0.025 N; $P = 0.004$). Egg albumin also had a notable impact on gel cohesiveness, with an effect of 0.019 N ($P = 0.014$), followed by calcium chloride (0.017 N; $P = 0.018$). A significant negative effect with sodium chloride (−0.018 N·s; $P = 0.016$), indicating that excessive levels of this monovalent salt reduced gel cohesiveness. Figure 4 (C) illustrates the standardized effects of the independent variables temperature, sucrose, and pH, all of which also had a significant impact, although to a lesser

 doi:10.20944/preprints202507.0021.v1

extent. Furthermore, the standardized effect of curvatures suggests that the study ranges for the independent variables were appropriately defined.

Regarding the viscosity index, data varied between 0.067 and 0.810 N·s, with the primary effects attributed to XG (0.409 N·s; $P < 0.001$), egg albumin (0.158 N·s; $P = 0.002$), FPM (0.150 N·s; $P = 0.002$), and calcium chloride (0.082 N·s; $P = 0.031$). Negative effects were observed with sucrose (−0.148 N·s; $P = 0.002$), sodium chloride (−0.119 N·s; $P = 0.007$), and temperature (−0.083 N·s; $P = 0.030$). Other independent variables (whey and soy proteins, carboxymethylcellulose, and pH) did not show significant effects on the viscosity index (Figure 4 (D)). The ANOVA showed a determination coefficient of 98.20%, with a significance level below 0.001 and a F_{calc} value 9.38 times greater than $F_{tab(12;6;0.10)}$. Analysis of the curvatures revealed significant effects on both responses, indicating that the ranges for the minimum and maximum limits of the independent variables were appropriately defined.

Discussion on the instrumental texture of gels. The results obtained for instrumental texture can be attributed to the gelling capacity of XG, which creates a stable three-dimensional structure that contributes to the development of firmer and more cohesive gels with greater resistance to deformation [69]. Its interaction with FPM further enhances this effect, which is auxiliary in reinforcing the gel structure through its colligative properties and intermolecular and intramolecular cohesion.

Plant-derived mucilage is notable for its high water retention capacity, emulsifying properties, and gel-forming abilities, making it a promising fat substitute in various food products [70]. In addition to the aforementioned polysaccharides, carboxymethylcellulose is commonly used as a thickener and stabilizer. However, its ability to form firm and cohesive gels is more limited compared to other hydrocolloids, such as XG.

Salts have a significant impact on the cohesiveness and viscosity index of gels because of their ability to influence intermolecular interactions and the structure of the gel network [71]. Monovalent ions, such as Na^+ in sodium chloride, neutralize the negative charges of proteins and anionic polysaccharide groups, reducing electrostatic repulsion and promoting closer molecular interactions, thus increasing the cohesiveness. This effect is more pronounced for the cation (Na^+) than the anion (Cl^-), as Na^+ has a smaller atomic radius and higher polarity, contributing to its stronger ionic strength compared to Cl^-.

In contrast, divalent ions like Ca^{2+} in calcium chloride ($CaCl_2$) form more intense ionic interactions with functional groups, particularly in proteins, which promote cross-linking and further enhance the cohesiveness of the gel network [72,73]. Both salts compete with other components for water, directly influencing the viscosity index [74].

Sugar positively affects the response of the viscosity index due to its interaction with water. This interaction increases the density of the solution, limiting the movement of water molecules and contributing to higher viscosity and mechanical resistance of the system [75]. Additionally, palm mucilage significantly enhances both the cohesiveness and viscosity index of the gel, due to its hydrodynamic properties, such as its high water retention capacity and ability to form structured three-dimensional networks, which provide greater stability and consistency to the gel matrix [76].

3.4. Chemometric Analysis

The heat map (Figure 5 (A)) highlighted a higher contribution of trials #1, #6, #8, and #10 to the gel texture data, as indicated by the yellowish color in the graph. Trial #12 also showed a similar effect, albeit with less intensity for consistency. These trials corresponded to the highest concentrations of XG (+1 = 1.8% w/w), a factor that influenced both gel texture and, to a lesser extent, rheological properties.

Preprints.org (www.preprints.org) | NOT PEER-REVIEWED | Posted: 1 July 2025 doi:10.20944/preprints202507.0021.v1

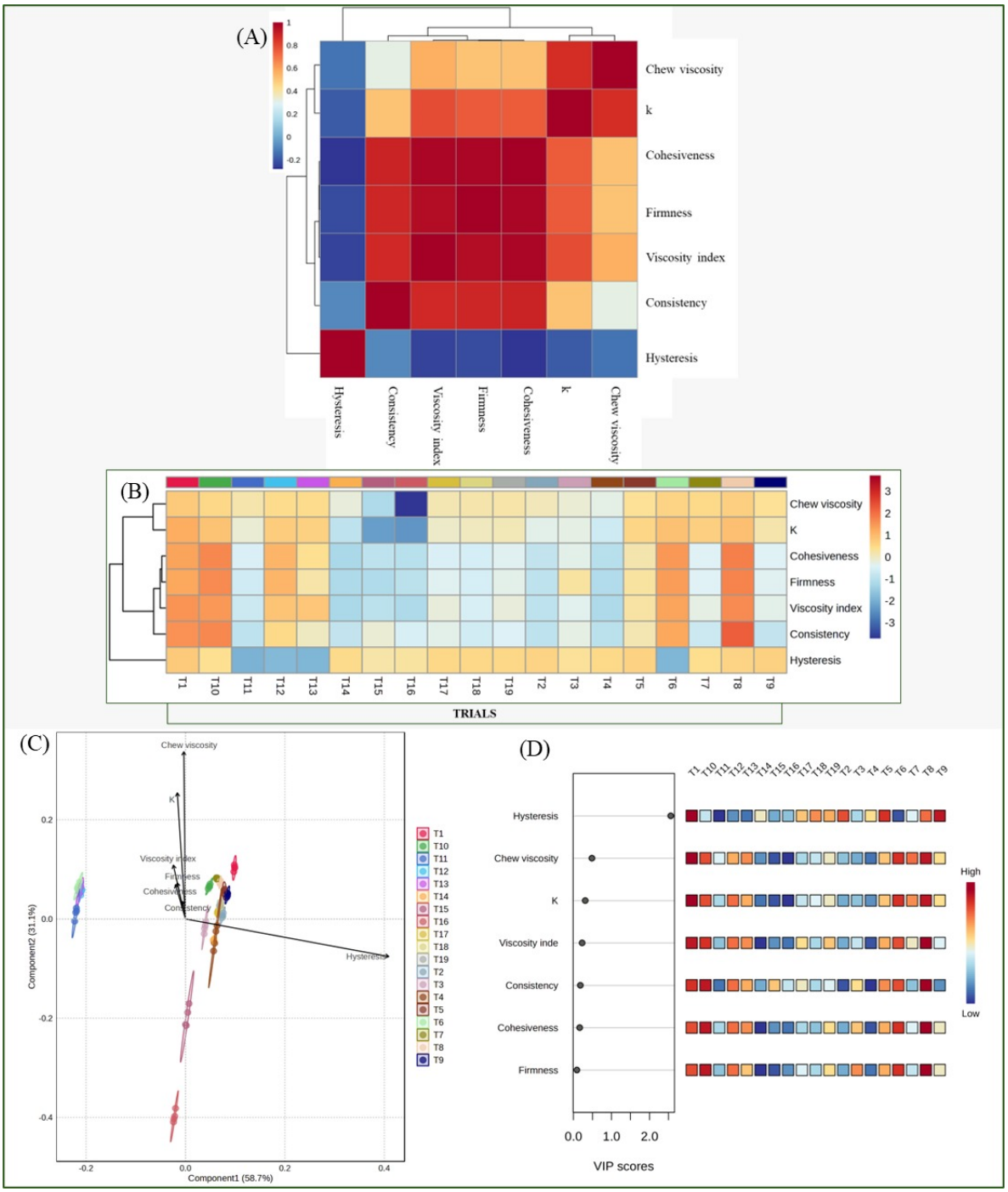

Figure 5. Graphical representation of the heat map (A), correlation analysis between the rheological and instrumental texture parameters (B), the scores of the principal component analysis (C) and Partial Least Squares Discriminant Analysis (PLS-DA) (D) of the gels obtained for the Plackett-Burman screening design trials.

In contrast, trials #15 and #16 demonstrated a pronounced effect in reducing the ascending and descending areas of the apparent viscosity curves, aligning with the lowest levels of independent variables. Trial #16, in particular, exhibited a similar effect on chewiness viscosity. Furthermore, the formulation and processing conditions of trials #6, #11,#12, and #13 favored the hysteresis area, which was consistent with the observations made for this dependent variable in the discussion.

The correlation between the dependent variables is represented by Pearson's correlation (Figure 5 (B)). A stronger interdependence was observed between rheological responses, as well as between instrumental texture responses (indicated by red areas). A weaker, though still positive, correlation was found between rheological and texture properties, except for hysteresis, which showed

 doi:10.20944/preprints202507.0021.v1

a negative correlation with all analyzed responses (shown in blue areas). Among instrumental texture properties, a higher correlation was noted between firmness, cohesiveness, and viscosity index. Similarly, for the rheological properties, this behavior was particularly evident between the ascending and descending areas.

The total variability of the experimental data was explained by 91.69% in the principal component analysis, with principal component 1 accounting for 97.98% and principal component 2 for 33.71%. The most prominent feature observed in principal component 1 was the influence of trials #6, #11, #12, and #13 (highlighted by the green ellipse) on the hysteresis results, as shown in Figure 5 (C). Furthermore, the cumulative impact of trials #15 and #16 on the viscosity properties of the chewiness was observed, along with the ascending and descending areas of the apparent viscosity curves, further confirming the results presented in the heat map.

The highest relative importance of the trials was observed for chewiness viscosity, with variable importance projection (VIP scores) above 1.6 (indicating the highest loading weights), as revealed by partial least squares discriminant analysis (Figure 5 (D)). These scores measure the overall contribution of each variable to the variance explained by all components. A score below 0.8 is considered less important, while values above 0.8 are highly relevant for regression models [77,78].

The behavior of trials #6, #11, #12, and #13 on hysteresis is depicted in Figure 5 (D) (blue areas), aligning with the results from the principal component analysis. This effect is considered beneficial for the development of gels intended for 3D food printing, as it supports flexibility in handling viscoelastic formulations that can potentially meet both the nutritional and sensory demands of modern consumers [24].

4. Conclusions

On the basis of the results obtained from the Plackett-Burman screening design, the most influential factors affecting the rheological behavior and texture of the studied gels were identified. XG emerged as the primary component responsible for increasing the viscosity and cohesiveness of the system because of its ability to form stable three-dimensional networks in an aqueous medium. However, palm mucilage also played an important role, serving as a crucial auxiliary in the enhancement of these properties. Palm mucilage exhibited physicochemical characteristics that favor water retention and the formation of structural bonds within the gel, contributing to greater stability and uniformity of the matrix.

Furthermore, its interaction with XG amplified the positive effects, demonstrating a synergistic behavior that further improved the cohesiveness and viscosity of the gel. These findings underscore the importance of strategically incorporating palm mucilage in formulation planning, particularly when optimizing properties such as firmness, cohesiveness, and resistance to flow. The gels studied present technofunctional characteristics relevant for application in 3D food printing or as a fat replacement in food matrix formulations. Identification of mucilage as a significant factor enhances its potential value in industrial applications, either as a complementary functional agent or as a sustainable alternative to other commonly used hydrocolloids. Therefore, the combined use of XG and palm mucilage presents a promising approach to developing products with improved rheological and sensory characteristics, meeting the needs of various industries, including food and pharmaceuticals."

Author Contributions: Conceptualization: N. A. N., L. O. F. R., M. P. D. A., T. N. A., M. S. Data curation: K. A. L., N. A. N., C. A. R.-C., G. P. C., S. L. R. M., T. N. A., M. T. P. S. C., M. S. Formal analysis: S. M. R., K. A. L., T. M. S., G. F. R. N., M. L. G. V., G. P. C., M. S. Funding acquisition: N. A. N., L. O. F. R., M. P. D. A., V. M. B., T. N. A., M. S. Investigation: S. M. R., K. A. L., C. A. R.-C., S. L. R. M., P. M. O., L. O. F. R., M. P. D. A., V. M. B., T. N. A., M. T. P. S. C., M. S. Methodology: S. M. R., K. A. L., T. M. S., G. F. R. N., M. L. G. V., G. P. C., V. M. B., T. N. A., M. S. Project administration: N. A. N., T. N. A., M. S. Resources: N. A. N., P. M. O., T. N. A., M. T. P. S. C., M. S. Supervision: T. N. A., M. T. P. S. C., M. S. Validation: K. A. L., S. L. R. M., L. O. F. R., M. P. D. A., T. N. A., M. S. Visualization: S. M. R., K. A. L., T. M. S., G. F. R. N., M. L. G. V., N. A. N., C. A. R.-C., G. P. C., P. M. O., L. O. F. R., M. P. D. A., V. M. B.,

 doi:10.20944/preprints202507.0021.v1

T. N. A., M. T. P. S. C., M. S. Writing – original draft preparation: S. M. R., K. A. L., T. M. S., N. A. N. Writing – review and editing: N. A. N., T. N. A., M. T. P. S. C., M. S.

Funding: This research was funded by the National Council for Scientific and Technological Development (CNPq) through financial support (#421777/2021-4) and by the Coordination for the Improvement of Higher Education Personnel (CAPES) through financial support (#001).

Institutional Review Board Statement: Not applicable.

Informed Consent Statement: Not applicable.

Data Availability Statement: All the data presented in this study are available in this article.

Acknowledgments: To the National Council for Scientific and Technological Development (CNPq) for the scholarships awarded to G.F.R.N (#173012/2024-8) and M.L.G.V (#172885/2024-8) and for the productivity grant to M.T.P.S.C. (#312786/2020-4) and to M. S. (#312759/2025-8). To the Research Support Foundation of the State of Minas Gerais (FAPEMIG) for the scholarships granted to S.M.R. (#14510) and T.M.S. (#77597). To the Agricultural Research Company of Minas Gerais (EPAMIG) from the Acauã experimental field for donating the forage palm. To the Institute of Science and Technology and the Federal University of Jequitinhonha and Mucuri Valleys for institutional support.

Conflicts of Interest: The authors declare no conflicts of interest. The funders had no role in the design of the study; in the collection, analyses, or interpretation of data; in the writing of the manuscript; or in the decision to publish the results.

Abbreviations

The following abbreviations are used in this manuscript:

ANOVA	analysis of variance
CMC	carboxymethyl cellulose
FPM	forage palm mucilage
SPI	soy protein isolate
XG	xanthan gum

References

1. Di Bella, G.; Lo Vecchio, G.; Albergamo, A.; Nava, V.; Bartolomeo, G.; Macrì, A.; Bacchetta, L.; Lo Turco, V.; Potortì, A. G. Chemical characterization of Sicilian dried nopal [Opuntia ficus-indica (L.) Mill.]. *J. Food Compos. Anal.* **2022**, *106*, 104307. https://doi.org/10.1016/j.jfca.2021.104307.
2. Santos, D. C.; Silva, M. C.; Alves, F. A. L.; Freitas, E. V. Botânica e cultivares. In *Palma forrageira: do plantio à colheita*; Donato, S. L. R.; Borém, A.; Rodrigues, M. G. V., Eds.; Epamig: Brasil, 2020; pp. 21–41.
3. Silva, L. E. P.; Moreira, S. R.; Neves, N. A.; Aguiar, E. V.; Capriles, V. D.; Amaral, T. N.; Schmiele, M. Use of integral forage palm flour as an innovative ingredient in new fettuccine-type pasta: Thermomechanical and technological properties, and sensory acceptance. *Foods* **2024**, *13*, 2683. https://doi.org/10.3390/foods13172683.
4. Macêdo, A. J. S.; Cesar Neto, J. M.; Oliveira, L. B.; Edvan, R. L.; Santos, E. M. The cactus pear culture, origin, introduction, expansion, utilities and future perspectives: Literature review. *Braz. J. Dev.* **2020**, *6*, 62967–62987. https://doi.org/10.34117/bjdv6n8-652.
5. Souza, G. F. A.; Pereira, M. M. L.; Silva, A. A. P.; Capuzzo, V. M. S.; Machado, F. Opuntia ficus-indica mucilage: A sustainable bio-additive for cementitious materials. *Constr. Build. Mater.* **2024**, *456*, 139254. https://doi.org/10.1016/j.conbuildmat.2024.139254.
6. Tosif, M. M.; Bains, A.; Goksen, G.; Rehman, M. Z.; Ali, N.; Karabulut, G.; Chawla, P. A comparative study on utilization of different plant-derived nano-mucilage as a fat replacer in yogurt: Product optimization, physicochemical attributes, shelf-life evaluation, and consumer perception with market orientation. *Food Chem. X* **2024**, *24*, 101920. https://doi.org/10.1016/j.fochx.2024.101920.
7. Santana, R. D. C.; Tavares, M. B.; Coimbra, J. S. D. R.; Martins, M. A.; Sousa, R. D. C. D. Effect of extraction conditions of chia (Salvia hispanica L.) mucilage on its chemical, rheological, and emulsifying properties. *ACS Food Sci. Technol.* **2025**, *5*, 687–694. https://doi.org/10.1021/acsfoodscitech.4c00845.

 doi:10.20944/preprints202507.0021.v1

8. Teotônio, D. O.; Rodrigues, S. M.; Leoro, M. G. V.; Pereira, P. A. P.; Schmiele, M. Potentialities of using cryoprotectants in gluten-free frozen dough and microwave baking as an emerging technology. *Res. Soc. Dev.* **2021**, *10*, e12410615674. https://doi.org/10.33448/rsd-v10i6.15674.
9. Lozano, E.; Padilla, K.; Salcedo, J.; Arrieta, A.; Andrade-Pizarro, R. Effects of yam (Dioscorea rotundata) mucilage on the physical, rheological and stability characteristics of ice cream. *Polymers* **2022**, *14*, 3142. https://doi.org/10.3390/polym14153142.
10. Felisberto, M. H. F.; Wahanik, A. L.; Gomes-Ruffi, C. R.; Clerici, M. T. P. S.; Chang, Y. K.; Steel, C. J. Use of chia (Salvia hispanica L.) mucilage gel to reduce fat in pound cakes. *LWT-Food Sci. Technol.* **2015**, *63*, 1049–1055. https://doi.org/10.1016/j.lwt.2015.03.114.
11. Schmiele, M.; Mascarenhas, M. C. C. N.; Barretto, A. C. S.; Pollonio, M. A. R. Dietary fiber as fat substitute in emulsified and cooked meat model system. *LWT-Food Sci. Technol.* **2015**, *61*, 105–111. https://doi.org/10.1016/j.lwt.2014.11.037.
12. Beikzadeh, S.; Khezerlou, A.; Jafari, S.; Pilevar, Z.; Mortazavian, A. Seed mucilages as the functional ingredients for biodegradable films and edible coatings in the food industry. *Adv. Colloid Interface Sci.* **2020**, *280*, 102164. https://doi.org/10.1016/j.cis.2020.102164.
13. Carvalho, H. J. M.; Souza, S. M.; Carvalho, C. W. P.; Nabeshima, E. H.; Schmiele, M. Cocoyam is an unconventional, innovative, and sustainable source of starch with potential use in sleek and functional biodegradable films. *Starch-Stärke* **2024**, Online version: 2400125. https://doi.org/10.1002/star.202400125.
14. Rooyen, B. V.; Wit, M.; Osthoff, G.; Niekerk, V. Cactus pear mucilage (Opuntia spp.) as a novel functional biopolymer: Mucilage extraction, rheology and biofilm development. *Polymers* **2024**, *16*, 1993. https://doi.org/10.3390/polym16141993.
15. Capitani, M.; Corzo-Ríos, L.; Chel-Guerrero, L.; Betancur-Ancona, D.; Nolasco, S.; Tomás, M. Rheological properties of aqueous dispersions of chia (Salvia hispanica L.) mucilage. *J. Food Eng.* **2015**, *149*, 70–77. https://doi.org/10.101/10.1016/j.jfoodeng.2014.09.043.
16. Geethalaxmi, M.; Sunil, C. K.; Venkatachalapathy, N. Tamarind seed polysaccharides, proteins, and mucilage: extraction, modification of properties, and their application in food. *Sustainable Food Technol.* **2024**, *2*, 1670–1685. https://doi.org/10.1039/d4fb00224e.
17. Lopes, A. C.; Ribas, M. F.; Tonial, I. B.; Lucchetta, L. Chia mucilage application (Salvia hispanica L.) in biscuit processing. *Braz. J. Dev.* **2020**, *6*, 17997–18008. https://doi.org/10.34117/bjdv6n4-100.
18. Cakmak, H.; Ilyasoglu-Buyukkestelli, H.; Sogut, E.; Ozyurt, V. H.; Gumus-Bonacina, C. E.; Simsek, S. A review on recent advances of plant mucilages and their applications in food industry: Extraction, functional properties and health benefits. *Food Hydrocoll. Health* **2023**, *3*, 100131. https://doi.org/10.1016/j.fhfh.2023.100131.
19. Aftab, K.; Hameed, S.; Umbreen, H.; Ali, S.; Rizwan, M.; Alkahtani, S.; Abdel-Daim, M. M. Physicochemical and functional potential of hydrocolloids extracted from some Solanaceae plants. *J. Chem.* **2020**, 563945. https://doi.org/10.1155/2020/3563945.
20. Goksen, G.; Demir, D.; Dhama, K.; Kumar, M.; Shao, P.; Xie, F.; Echegaray, N.; Lorenzo, J. M. Mucilage polysaccharide as a plant secretion: Potential trends in food and biomedical applications. *Int. J. Biol. Macromol.* **2023**, *230*, 123146. https://doi.org/10.1016/j.ijbiomac.2023.123146.
21. Guo, J.; Gu, X.; Meng, Z. Customized 3D printing to build plant-based meats: Spirulina platensis protein-based Pickering emulsion gels as fat analogs. *Innov. Food Sci. Emerg. Technol.* **2024**, *94*, 103679. https://doi.org/10.1016/j.ifset.2024.103679.
22. Caulier, S.; Doets, E.; Noort, M. An exploratory consumer study of 3D printed food perception in a real-life military setting. *Food Qual. Prefer.* **2020**, *86*, 104001. https://doi.org/10.1016/j.foodqual.2020.104001.
23. Nadagouda, M. N.; Ginn, M.; Rastogi, V. A review of 3D printing techniques for environmental applications. *Curr. Opin. Chem. Eng.* **2020**, *28*, 173–178. https://doi.org/10.1016/j.coche.2020.08.002.
24. Lourenço, M.; Clerici, M. T. P. S.; Silva, L. R.; Nolasco, M. V. F. M. 3D food printing: A review of history, functionality and challenges in product development. *Res. Soc. Dev.* **2025**, *14*, e1714147902. https://doi.org/10.33448/rsd-v14i1.47902.
25. Yang, X.; Li, A.; Li, D.; Guo, Y.; Sun, L. Applications of mixed polysaccharide-protein systems in fabricating multi-structures of binary food gels—A review. *Trends Food Sci. Technol.* **2021**, *109*, 197–210. https://doi.org/10.1016/j.tifs.2021.01.002.
26. Wang, P.; Liao, Q.; Zhang, H. Polysaccharide-based double-network hydrogels: Polysaccharide effect, strengthening mechanisms, and applications. *Biomacromolecules* **2023**, *24*, 5479–5510. https://doi.org/10.1021/acs.biomac.3c00765.

 doi:10.20944/preprints202507.0021.v1

27. Guan, C.; Wang, C.; Fu, S. Food protein nanofibril gels: From conditions, types and properties to applications. *Foods* **2024**, *13*, 2173. https://doi.org/10.3390/foods13142173.
28. Tang, Q.; Roos, Y. H.; Miao, S. Structure, gelation mechanism of plant proteins versus dairy proteins and evolving modification strategies. *Trends Food Sci. Technol.* **2024**, *147*, 104464. https://doi.org/10.1016/j.tifs.2024.104464.
29. Li, M.; Feng, L.; Xu, Y.; Nie, M.; Li, D.; Zhou, C.; Dai, Z.; Zhang, Z.; Zhang, M. Rheological property, β-carotene stability and 3D printing characteristic of whey protein isolate emulsion gels by adding different polysaccharides. *Food Chem.* **2023**, *414*, 135702. https://doi.org/10.1016/j.foodchem.2023.135702.
30. Kazemi-Taskooh, Z.; Varidi, M. How can plant-based protein–polysaccharide interactions affect the properties of binary hydrogels? (A review). *Food Funct.* **2023**, *14*, 5891–5909. https://doi.org/10.1039/D3FO00611E.
31. Makshakova, O. N.; Zuev, Y. F. Interaction-induced structural transformations in polysaccharide and protein-polysaccharide gels as functional basis for novel soft-matter: A case of carrageenans. *Gels* **2022**, *8*, 287. https://doi.org/10.3390/gels8050287.
32. AOAC. *Official Methods of Analysis of AOAC International*, 22nd ed.; Association of Official Analysis Chemists International: Gaithersburg, USA, 2023.
33. Zhai, W.; Bao, S.; Han, R.; Wang, C.; He, J.; Zhong, F.; Xia, Y. Impact of reduced sucrose content on processed cheese: Sensory, textural, and storage stability analysis. *Food Biosci.* **2024**, *60*, 104405. https://doi.org/10.1016/j.fbio.2024.104405.
34. Sapper, M.; Talens, P.; Chiralt, A. Improving functional properties of cassava starch-based films by incorporating xanthan, gellan, or pullulan gums. *Int. J. Polym. Sci.* **2019**, 367164. https://doi.org/10.1155/2019/5367164.
35. Yar, M. S.; Ibeogu, I. H.; Bako, H. K.; Alnadari, F.; Bilal, M.; Rehman, F.; Zhu, J.; Zhou, T.; Zhao, Z.; Li, C. A novel carboxymethyl cellulose/gum xanthan and citric acid-based film that enhances the precision of blackcurrant anthocyanin-induced color detection for beef spoilage tracking. *Food Chem.* **2024**, *461*, 140905. https://doi.org/10.1016/j.foodchem.2024.140905.
36. Yang, S.; Zheng, B.; Huang, L.; Zhang, Y.; Zeng, H. Saltiness perception mechanism and salt reduction strategies in food. *Trends Food Sci. Technol.* **2024**, *148*, 104521. https://doi.org/10.1016/j.tifs.2024.104521.
37. Alavi, F.; Tian, Z.; Chen, L.; Emam-Djomeh, Z. Effect of $CaCl_2$ on the stability and rheological properties of foams and high-sugar aerated systems produced by preheated egg white protein. *Food Hydrocoll.* **2020**, *106*, 105887. https://doi.org/10.1016/j.foodhyd.2020.105887.
38. Sepúlveda, F.; Oyarzun-Ampuero, F.; Matiacevich, S.; Ortiz-Viedma, J.; Lemus-Mondaca, R.; Char, C. Use of whey protein concentrates to encapsulate hydrophobic natural antimicrobials to improve their incorporation into high-moisture foods enhancing their antimicrobial activity. *Innovative Food Sci. Emerg. Technol.* **2024**, *94*, 103687. https://doi.org/10.1016/j.ifset.2024.103687.
39. Yang, Y.; Meng, J.; Lei, L.; Huang, D.; Liu, C.; Gu, D.; Ito, Y. Different behavior of bovine serum albumin as foaming agent in foam enrichment of Rhodamine 6G and Evans blue. *Sep. Purif. Technol.* **2020**, *252*, 117509. https://doi.org/10.1016/j.seppur.2020.117509.
40. Liang, G.; Chen, W.; Zhang, X.; Zeng, M.; Qin, F.; He, Z.; Goff, H. D.; Chen, J.; Wang, Z. Incorporating soy protein hydrolysate and temperature-induced gelling polysaccharide as partial egg replacements for enhanced texture in sponge cake. *Food Biosci.* **2024**, *57*, 103574. https://doi.org/10.1016/j.fbio.2024.103574.
41. Rodrigues, M. I.; Iemma, A. F., Eds. *Experiment Design and Process Optimization*; CRC Press: USA, 2014.
42. Riquelme, N., Savignones, C., López, A., Zúñiga, R. N., & Arancibia, C. (2023). Effect of gelling agent type on the physical properties of nanoemulsion-based gels. *Colloids and Interfaces*, **7**(3), 49. https://doi.org/10.3390/colloids7030049
43. Massaretto, I. L.; Meza, S. L. R.; Schmiele, M.; Marquez, U. M. L.; Sinnecker, P. Nutritional characterization and effect of cooking on phenolic compounds, antioxidant capacity and sensory acceptability of commercial wild rice (Zizania aquatica L.). *Biocatal. Agric. Biotechnol.* **2023**, *50*, 102705. https://doi.org/10.1016/j.bcab.2023.102705.
44. Silva, I. L.; Silva, L. A. O.; Coelho, L. C. B. B. The Brazilian Caatinga biome and its biotechnological potential. In *Advances in Applied Science and Technology*; Teodor, R., Ed.; BP International: Índia, 2019; pp 123–142.
45. Giura, L., Urtasun, L., Belarra, A., Ansorena, D., & Astiasarán, I. (2021). Exploring tools for designing dysphagia-friendly foods: A review. *Foods*, **10**(6), 1334. https://doi.org/10.3390/foods10061334
46. Costa, R.S., Costa, R.M.R., & Silva Júnior, J.O.C. (2021). Rheological behavior and antimicrobial activity of a topical formulation containing extract of *Heliotropium indicum* L. *Research, Society and Development*, **10**, e32310515068. https://doi.org/10.33448/rsd-v10i5.15068

 doi:10.20944/preprints202507.0021.v1

47. Mathias, T.R.S., Andrade, K.C.S., Rosa, C.L.S., & Silva, B.A. (2013). Rheological evaluation of different commercial yoghurts. *Brazilian Journal of Food Technology*, **16**, 12–20. https://doi.org/10.1590/S1981-67232013005000004
48. Yu, J., Wang, Y., Li, D., & Wang, L.-J. (2022). Freeze–thaw stability and rheological properties of soy protein isolate emulsion gels induced by NaCl. *Food Hydrocolloids*, 123, 107113. https://doi.org/10.1016/j.foodhyd.2021.107113
49. Kumar, P., Kumar, B., Gihar, S., & Kumar, D. (2024). Review on emerging trends and challenges in the modification of xanthan gum for various applications. *Carbohydrate Research*, **538**, 109070. https://doi.org/10.1016/j.carres.2024.109070
50. Meydanju, N., Pirsa, S., & Farzi, J. (2022). Biodegradable film based on lemon peel powder containing xanthan gum and TiO_2–Ag nanoparticles: Investigation of physicochemical and antibacterial properties. *Polymer Testing*, **106**, 107445. https://doi.org/10.1016/j.polymertesting.2021.107445
51. Pirsa, S., & Hafezi, K. (2023). Hydrocolloids: Structure, preparation method, and application in food industry. *Food Chemistry*, **399**, 133967. https://doi.org/10.1016/j.foodchem.2022.133967
52. Zheng, Z., Sun, Z., Li, M., Yang, J., Yang, Y., Liang, H., Xiang, H., Meng, J., Zhou, X., Liu, L., Wu, Z., & Yang, S. (2024). An update review on biopolymer xanthan gum: Properties, modifications, nanoagrochemicals, and its versatile applications in sustainable agriculture. *International Journal of Biological Macromolecules*, **281**, 136562. https://doi.org/10.1016/j.ijbiomac.2024.136562
53. Hassanisaadi, M., Vatankhah, M., Kennedy, J.F., Rabiei, A., & Riseh, R.S. (2025). Advancements in xanthan gum: A macromolecule for encapsulating plant probiotic bacteria with enhanced properties. *Carbohydrate Polymers*, **348**, 122801. https://doi.org/10.1016/j.carbpol.2024.122801
54. Han, C., Feng, G., Yin, S., Wang, G., Wang, J., Wan, Z., Guo, J., & Yang, X. (2024). Stabilization of oil-water interface by non-interfacial adsorbed native starch granules using depletion attraction. *Food Hydrocolloids*, **156**, 110330. https://doi.org/10.1016/j.foodhyd.2024.110330
55. Hou, J., Liu, Y., Jiang, Z., Chuang, R., Zhang, H., Li, H., Xia, N., Ma, Y., Zheng, L., Rayan, A. M., Ghamry, M., & Qin, D. (2025). Charge density of carboxymethyl cellulose affects depletion attraction-stabilized egg yolk Pickering emulsion gels: Rheological and interfacial properties. *Food Hydrocolloids*, **159**, 110612. https://doi.org/10.1016/j.foodhyd.2024.110612
56. Jia, W., Cui, B., Ye, T., Lin, L., Zheng, H., Yan, X., Li, Y., Wang, L., Liu, S., & Li, B. (2014). Phase behavior of ovalbumin and carboxymethylcellulose composite system. *Carbohydrate Polymers*, **109**, 64–70. https://doi.org/10.1016/j.carbpol.2014.03.026
57. Medeiros, V. P. B., Oliveira, K. Á. R., Queiroga, T. S., & Souza, E. L. (2024). Development and application of mucilage and bioactive compounds from Cactaceae to formulate novel and sustainable edible films and coatings to preserve fruits and vegetables—A review. *Foods*, **13**, 3613. https://doi.org/10.3390/foods13223613
58. Goto, T., Shimamoto, S., Takaya, M., Sato, S., Takahashi, K., Nishimura, K., Morii, Y., Kunishige, K., Ohtsuka, A., & Ijiri, D. (2021). Impact on genetic differences among various chicken breeds on free amino acid contents of egg yolk and albumen. *Scientific Reports*, **11**, 2270. https://doi.org/10.1038/s41598-021-81660-3
59. Muhedaner, M., Bako, H.K., Zhou, G., & Ye, K. (2025). Impact of egg white protein on mycoprotein gel: Insights into rheological properties, protein structure and molecular interactions. *Food Chemistry*, **463**, 141366. https://doi.org/10.1016/j.foodchem.2024.141366
60. Zhang, M., Mei, L., Wu, Y., Jin, G., & Bao, D. (2024). Impact of ethanol extract of propolis on heat-induced egg white protein gels: Formation and properties. *Food Hydrocolloids*, **149**, 109590. https://doi.org/10.1016/j.foodhyd.2023.109590
61. Lopez, C.G., & Richtering, W. (2021). Oscillatory rheology of carboxymethyl cellulose gels: Influence of concentration and pH. *Carbohydrate Polymers*, **267**, 118117. https://doi.org/10.1016/j.carbpol.2021.118117
62. Shibaev, A.V., Muravlev, D.A., Muravleva, A.K., Matveev, V.V., Chalykh, A.E., & Philippova, O.E. (2020). pH-dependent gelation of a stiff anionic polysaccharide in the presence of metal ions. *Polymers*, **12**(4), 868. https://doi.org/10.3390/polym12040868
63. Lu, F., Chi, Y., & Chi, Y. (2024). Preparation of high internal phase emulsions based on high-temperature glycation-modified egg white protein: Structural characteristics, stability, and β-carotene bioavailability under multi-parameter regulation. *International Journal of Biological Macromolecules*, **283**, 137870. https://doi.org/10.1016/j.ijbiomac.2024.137870

 doi:10.20944/preprints202507.0021.v1

64. Zhao, Y.-R., Peng, N., Wang, C., Li, Y.-Q., Liang, Y., Guo, Z.-W., Sun, A.-Y., & Ren, X. (2024). Preparation and characterization of pea protein isolate-egg white protein composite gels. *Food Hydrocolloids*, **148**, 109464. https://doi.org/10.1016/j.foodhyd.2023.109464
65. Schmiele, M., Araújo, T.L., Gurgueira, M.D., & Chang, Y.K. (2015). Determination of the concentration of different solvents systems in the protein solubilization of meat analogue. *Ciência Rural*, **45**, 1120–1125. https://doi.org/10.1590/0103-8478cr20131630
66. Lima, C.T., Lima, N.G., Rodrigues, S.M., Neves, N.A., Meza, S.L.R., & Schmiele, M. (2022). Experimental optimization tool for the development of muffins with high technological and nutritional value using whole flours of rice, red sorghum and carioca bean. *Research, Society and Development*, **11**, e34111133337. https://doi.org/10.33448/rsd-v11i11.33337
67. Souza, E.C., Cordeiro, D.A., Silva, B.S., Neves, N.A., & Schmiele, M. (2022). Development of muffin with the incorporation of olive pomace flour, extra virgin olive oil and hydrolyzed soy protein. *Research, Society and Development*, **11**, e58511226012. https://doi.org/10.33448/rsd-v11i2.26012
68. Wang, X., Fei, W., Shen, M., Wen, H., Chen, F., & Xie, J. (2024). Texture, swallowing and digestibility characteristics of a low-GI dysphagia food as affected by addition of dietary fiber and anthocyanins. *Food Research International*, **197**, 115201. https://doi.org/10.1016/j.foodres.2024.115201
69. Cofelice, M., Messia, M.C., Marconi, E., Cuomo, F., & Lopez, F. (2023). Effect of the xanthan gum on the rheological properties of alginate hydrogels. *Food Hydrocolloids*, **142**, 108768. https://doi.org/10.1016/j.foodhyd.2023.108768
70. Amiri, M.S., Mohammadzadeh, V., Yazdi, M.E.T., Barani, M., Rahdar, A., & Kyzas, G.Z. (2021). Plant-based gums and mucilages applications in pharmacology and nanomedicine: A review. *Molecules*, **26**(6), 1770. https://doi.org/10.3390/molecules26061770
71. Chu, L., Yang, L., Li, J., Lin, L., & Zheng, G. (2019). Effect of *Smilax china* L. starch on the gel properties and interactions of calcium sulfate-induced soy protein isolate gel. *International Journal of Biological Macromolecules*, **135**, 127–132. https://doi.org/10.1016/j.ijbiomac.2019.05.130
72. Damodaran, S., & Parkin, K.L. (Eds.). (2017). *Fennema's Food Chemistry* (5th ed.). CRC Press: Boca Raton.
73. Wong, D.W.S. (2018). *Mechanism and Theory in Food Chemistry* (2nd ed.). Springer Cham: Switzerland.
74. Garcia, J., Moura, M., & Aouada, F. (2019). Effect of pH, ionic concentration and species on the absorption of water by hydrogel bionanocomposits constituted from CMC/PAAm/Laponite RDS. *Química Nova*, **42**, 831–837. https://doi.org/10.21577/0100-4042.20170396
75. Benítez, E. I., Genovese, D. B., & Lozano, J. E. (2009). Effect of typical sugars on the viscosity and colloidal stability of apple juice. *Food Hydrocolloids*, **23**, 519–525. https://doi.org/10.1016/j.foodhyd.2008.03.005
76. Monteiro, S. S., Queiroz, J. V. S. A., Gomes, H. M., Santos, L., Moreira, J. C. F., Gelain, D. P., Fook, M. V. L., Lisboa, H. M., & Pasquali, M. A. B. (2025). Characterization of mucilage from *Opuntia cochenillifera* cladodes: Rheological behavior, cytotoxicity, and antioxidant potential. *Colloids and Surfaces A: Physicochemical and Engineering Aspects*, **707**, 135824. https://doi.org/10.1016/j.colsurfa.2024.135824
77. Kumawat, K. L., Raina, S. K., Kumar, D., Verma, M. K., Singh, D., Mir, J. I., Sultan, S. M., & Sharma, O. C. (2024). Association of reproductive phenology with air temperature in almond (*Prunus dulcis* [Mill.] D.A. Webb) cultivars under northwestern Himalayan conditions. *Applied Fruit Science*, **66**, 581–588. https://doi.org/10.1007/s10341-023-00991-9
78. Ray, A., Ghosh, S., Ray, A., & Aswatha, S. M. (2015). An analysis of the influence of growth periods on potential functional and biochemical properties and thermal analysis of freeze-dried *Aloe vera* L. gel. *Industrial Crops and Products*, **76**, 298–305. https://doi.org/10.1016/j.indcrop.2015.05.015